

ELECTROSTATIC CORROSION ANALYSIS WITH DAMAGED PASSIVE FILM MODEL OF STAINLESS STEEL

O. KUWAZURU, K. ODE & W. LIU

Department of Nuclear Power & Energy Safety Engineering, University of Fukui, Japan

ABSTRACT

The corrosion electric field around the surface of stainless steel under tensile stress is addressed through the experiment and simulation. When the stress is applied, the passive film is locally damaged on the grain boundaries causing microscopic stress and strain concentrations. In a corrosive environment, the plastic strain induced by the strain concentration breaks the passive film and generates a new surface without the passive film. This causes a galvanic corrosion between the intact surface with passive film and the damaged surface without passive film. The effect of stress on the polarization curve was observed by electrochemical and mechanical experiments, and we found that the spontaneous potential decreased as the applied stress increased. To evaluate the electrochemical property of stressed stainless steel, the electric field analysis is formulated by the boundary element method (BEM) with the damaged passive film model and the empirical polarization curve model.

Keywords: boundary element method, electrochemistry, nonlinear boundary, passive film, potential problem, stainless steel, stress corrosion.

1 INTRODUCTION

Metal corrosion is a bothersome unresolved problem for machinery exposed to a natural environment and chemical or power plants containing a corrosive solution. Austenitic stainless steel is a superb material which has a superior corrosion-resistance and high fracture toughness. The corrosion-resistance arises from the passive film made of chromium oxide or chromium hydrated oxide [1]. If the film is damaged by some reason, it can be immediately and automatically reproduced unless the surface is prevented to react with oxygen in ambient air or noncorrosive solutions. However, when the stainless steel is subjected to a stress in a corrosive environment, a mechanical damage of passive film is caused by a microscopic plastic deformation around the grain boundaries, which cannot be repaired due to the existence of active anions such as chlorine ion in an electrolyte solution that prevent the regeneration of oxide film [1]. Consequently, the corrosion develops selectively on the damaged portion and leads to a pitting corrosion and finally causes a stress corrosion cracking (SCC). The corrosion fatigue (CF) also develops in a similar manner. Hence, the corrosion behaviour is important to evaluate the initiation of SCC or CF. Meanwhile, it is not easy to quantitatively evaluate the corrosion rate and the generation of corrosion pits on the surface of stressed stainless steels. Therefore, the quantitative evaluation method using a numerical simulation to consider the complicated phenomena of metal corrosion under mechanical stress is desired to be established.

The corrosion is a chemical reaction and its driving force is the electric potential of the metal surface. The typical type of corrosion is the galvanic corrosion where two different materials in contact with one another in a corrosive environment generate a potential gap between the two materials to enhance the chemical reactions on the anodic and cathodic surfaces. Since the rate of chemical reactions can be detected indirectly by the electric current, if the electric field can be evaluated exactly around the surface of materials, the corrosion rate can also be determined from the electric current. From such a viewpoint,

the electric field analysis of galvanic corrosion has been studied for a long time [2, 3], and the boundary element method (BEM) has been applied to practical corrosion problems by many researchers [4–10]. However, the effect of stress on the electrochemical property has not been included in the BEM formulation because of the difficulty to deal with the coupling effect of stress and corrosion, and a few studies have investigated the effect of stress on the polarization curve by the experiments [10–13] and tried to use in the BEM simulation [10].

Advantage of the BEM is not only the computational efficiency achieved by reducing the dimension of integration but also the ease in handling of a singularity or discontinuity of the field variables. In the corrosion problem, the electrostatic potential and current density is discontinuous on the border line between two different materials in contact on the boundary of analysis domain of the electrolyte solution by which the materials are dissolved. From this viewpoint, in this study, we employ the BEM with a discontinuous element [14, 15] to evaluate the electric potential and current density on the damaged surface of stainless steel. The damage is considered to be induced by the microscopic plastic deformation, and modelled by the loss of passive film. The electrochemical property of the intact stainless steel can be measured by the experiment. However, the electrochemical property of the damaged portion of stainless steel cannot be measured solely. Therefore, we assume that the damaged portion, which is a newly generated surface without the passive film, is similar to a surface of carbon steel for simplicity, and the electrochemical property of the damaged portion is substituted by that of carbon steel obtained by the experiment. For comparison with the numerical results, the effect of stress on the macroscopic (averaged) electrochemical property of the stainless steel is evaluated by the experiment. The comparison between numerical and experimental results demonstrates the validity of the damaged passive film model of stainless steel.

2 ELECTROCHEMICAL AND MECHANICAL TESTING

2.1 Materials and methods

The material used in the experiment is SUS316 austenitic stainless steel, and the corrosive environment is 1.0 mass% NaCl aqueous solution in room temperature. The electrochemical property is evaluated by the polarization curve which is the relationship between potential and current density. Moreover, the effect of tensile stress on the polarization curve is measured using the electrochemical and mechanical testing apparatus developed in this study, and its picture is shown in Fig. 1. The shape of tensile specimen is shown in Fig. 2, and the thickness is 3 mm. It has two holes to insert the pins by which the tension is applied, and a bolt hole on the one end to fix the lead wire to measure the electric potential and current of the specimen. The grey area including the side and back surfaces is coated by a nail polish, and the white area only on the front surface remains exposed to be subjected to corrosion. Before the coating, a lead wire is attached and a strain gauge is glued on the back surface. The size of this corrosion window is 3 mm × 3 mm.

The specimen is pulled via the locking pins by using the hydraulic servo fatigue testing machine. The specimen and fixation rigs are covered by the acrylic chamber filled partially with the NaCl solution where the specimen is fully immersed. The upper part of the chamber is slightly opened to move the upper rig without friction with the chamber. The polarization curve under constant stress is measured by the three electrodes connected to the potensio-



Figure 1: Testing apparatus with corrosion chamber mounted on hydraulic fatigue testing machine.

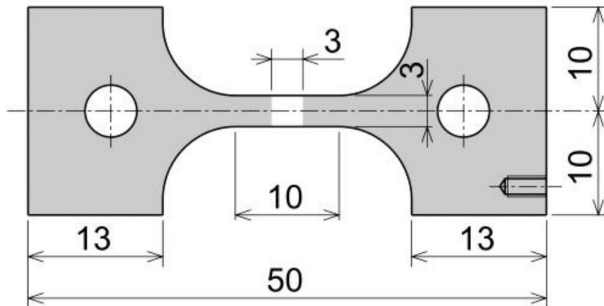


Figure 2: Shape of tensile specimen.

galvanostat VersaSTAT3-300 (Princeton Applied Research) with the potensio-dynamic mode of linear sweep. The working electrode is the tensile specimen, the counter electrode is a platinum wire, and the reference electrode is an Ag|AgCl electrode. The electric potential is measured as a relative potential to the reference electrode. The polarization curves in four cases are measured where the applied tensile stress is set to 0, 20, 200 and 300 MPa. The range of linear sweep is set from $-1,300$ to 700 mV vs. Ag|AgCl, and the sweep rate is 1 mV/s. One specimen is prepared for one stress condition, so totally four specimens are used.

2.2 Polarization curve under tensile stress

The obtained polarization curves are shown in Fig. 3, where the abscissa indicates the absolute current density in logarithmic scale and the ordinate indicates the potential difference

in linear scale. The level of leftward peak of the polarization curve means the spontaneous potential at which the current density is completely zero. The lower part below the spontaneous potential is the cathodic curve and the upper part is the anodic curve corresponding to the metal dissolution. The inflection point of anodic curve means the pitting potential over which the pitting corrosion occurs on the surface of stainless steel. As seen in Fig. 3, the effect of stress on the polarization curve is observed mainly on the spontaneous potential, which decreased as the applied constant stress increased.

In principle, the polarization curve means the activity of chemical reactions on the material surface. The decrease in the spontaneous potential described above comes from the variation of the surface condition, which is caused by the damage of passive film. The stress was uniformly applied to the specimen in the experiment. In microscopic sense, however, since the material has a metallographic heterogeneity consisting of polycrystalline grains, the stress nonuniformly distributes over the grains and concentrates on the grain boundaries. This concentrated high stress causes a plastic strain around the grain boundaries, and locally breaks the passive film. When the passive film is broken, a new surface is generated without the passive film. In the NaCl solution, the passivation of this new surface is prevented by Cl^- ions and, therefore it remains a different surface from the intact surface of passive film. Consequently, in the stressed condition, the surface of stainless steel consists of two types, that is, the intact passive film and damaged unoxidized surface. When the applied stress increases, the area of damaged surface also increases. Since the standard electrode potential of a steel without passive film is lower than the intact stainless steel [1], the increase in the damaged area leads to a decrease in the averaged potential of the whole surface. This is the reason why the spontaneous potential decreased as the applied stress increased in the above-mentioned experiment. The aim of this study is to quantitatively evaluate the corrosion behaviour on this kind of mechanically damaged surface of stainless steel.

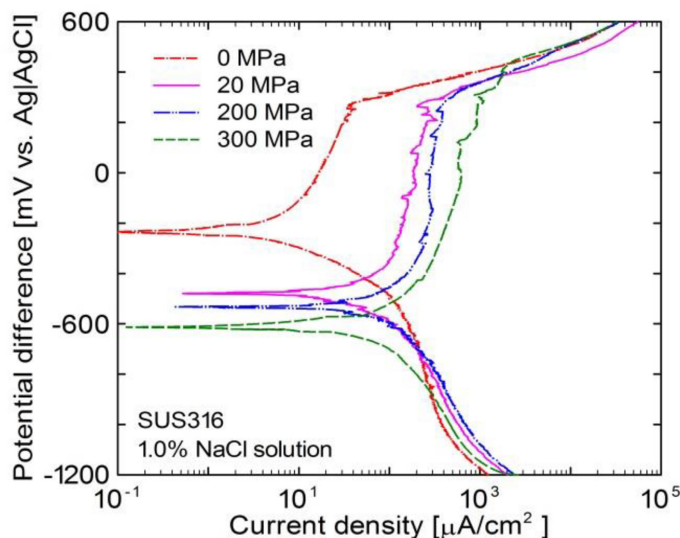


Figure 3: Polarization curves of SUS316 stainless steel under tensile stress.

3 CORROSION ELECTRIC FIELD SIMULATION

3.1 Boundary element formulation

The electric field of galvanic corrosion is described as a potential problem and can be solved by the BEM [4–10]. The analysis domain is the region filled by the electrolyte solution as shown in Fig. 4. Two-dimensional problem is assumed in this study. The potential problem is a linear problem but the corrosion problem has a nonlinear boundary condition described by the polarization curve. There are three types of boundaries, that is, Dirichlet boundary, Neumann boundary, and metal boundary. They are denoted by Γ_D , Γ_N and Γ_M , respectively. The electric potential is prescribed as $p = \underline{p}$ on Γ_D , and the outward electric current density is prescribed as $\hat{q} = \hat{\underline{q}}$ on Γ_N . Moreover, the metal boundary Γ_M is divided into two parts, that is, the anodic part Γ_A and cathodic part Γ_C as shown in Fig. 4. In a normal galvanic corrosion, the anode and cathode are different materials. However, in this study, they are both same material, but the damaged part and the intact part become the anode and cathode, respectively. Moreover, the external potential gap or electric current is applied by the Dirichlet or Neumann boundary, the chemical reaction on the metal surface may switch to cathodic or anodic reaction. For example, in the polarization experiment mentioned above, the lower potential than the spontaneous potential is applied on the surface, the cathodic reaction occurs even on the damaged part. In such sense, Γ_A and Γ_C vary and differ from the division of damaged and intact surfaces depending on the total potential balance, and the polarization curve including both the anodic and cathodic reactions is necessary to be assigned to the metal boundary. The polarization curves of damaged and intact surfaces are different, and the property of the damaged part cannot be measured directly in the experiment. Therefore, the polarization curve of the damaged surface is only approximately determined by the experimental data of a carbon steel as described below.

The potential problem is described by the Laplace equation of the electric potential p :

$$\kappa \nabla^2 p = 0. \quad (1)$$

The coefficient κ is the electric conductivity of the electrolyte solution. By employing the normal BEM formulation [14, 15] to eqn (1), we obtain the matrix equation:

$$[H]\{p\} = [G]\{\hat{q}\} \quad (2)$$

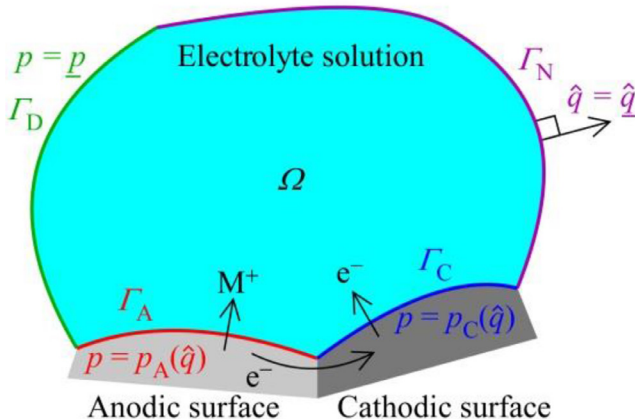


Figure 4: Boundary condition of corrosion electric field.

where $\{p\}$ is the nodal potential vector, $\{\hat{q}\}$ the nodal outward current density vector, $[H]$ and $[G]$ are the square constant coefficient matrices.

For nonlinear calculation, we define the residual vector as

$$\{R\} = [H]\{p\} - [G]\{\hat{q}\}. \quad (3)$$

Moreover, to consider the nonlinear boundary condition on the metal boundary Γ_M , the matrices and vectors in eqn (3) are separated to partial matrices and partial vectors based on the three boundary types as

$$\{R\} = [[H_D] \ [H_N] \ [H_M]] \begin{Bmatrix} \{p_D\} \\ \{p_N\} \\ \{p_M\} \end{Bmatrix} - [[G_D] \ [G_N] \ [G_M]] \begin{Bmatrix} \{\hat{q}_D\} \\ \{\hat{q}_N\} \\ \{\hat{q}_M\} \end{Bmatrix}. \quad (4)$$

$\{p_M\}$ is a nonlinear function of $\{\hat{q}_M\}$ obtained by the polarization curve mentioned above. For nonlinearity, all the nodal variables are divided into the current value and incremental value as

$$p_i = \bar{p}_i + \Delta p_i, \quad \hat{q}_i = \bar{\hat{q}}_i + \Delta \hat{q}_i \quad (5)$$

where p_i and \hat{q}_i are the potential and outward current density of i th node, \bar{p}_i and $\bar{\hat{q}}_i$ their current values, and Δp_i and $\Delta \hat{q}_i$ their increments. Then, assuming that the nodal potential p_i is determined locally by the nodal current density \hat{q}_i , the relationship between their increments is approximated in the linear form as

$$\Delta p_i = \frac{\partial p_i}{\partial \hat{q}_i} \Delta \hat{q}_i. \quad (6)$$

The value of partial differentiation is obtained from the polarization curve. Applying the incremental decomposition by eqns (4) and (5), and substituting the linearization by eqn (6), we obtain the linear simultaneous equations to be solved as

$$[-[G_D] \ [H_N] \ [D_M]] \begin{Bmatrix} \{\Delta \hat{q}_D\} \\ \{\Delta p_N\} \\ \{\Delta \hat{q}_M\} \end{Bmatrix} = \{\bar{R}\} - [H_D]\{\Delta p_D\} + [G_N]\{\Delta \hat{q}_N\}. \quad (7)$$

The partial matrix $[D_M]$ is determined by

$$[D_M] = [H_M] \left[\text{diag} \left(\frac{\partial p_i}{\partial \hat{q}_i} \right) \right] - [G_M] \quad (8)$$

and $\{\bar{R}\}$ is the current residual:

$$\{\bar{R}\} = [H]\{\bar{p}\} - [G]\{\bar{\hat{q}}\}. \quad (9)$$

By solving eqn (7) iteratively, the nonlinear solution can be obtained as a converged value. On the metal boundary Γ_M , the initial value of current density is set to zero to calculate the initial coefficient matrices. As described earlier, the potential and current density are discontinuous on the border point between two materials; therefore, we use the discontinuous linear element [14, 15].

3.2 Passive film model

Since the actual detailed condition of microscopic damage on the surface of stainless steel is unknown, a simplified damage model is used in this numerical example. Let us consider a rectangular domain of analysis as shown in Fig. 5. The metal boundary is located on the bottom of domain, and a periodic microscopic damaged surface is assumed. A single unit of length l has a damaged surface of length r in its centre. This unit is repeated, and totally N_r units are assumed on the metal boundary. The length of damaged surface r is considered to represent the plastic strain $\varepsilon_p = r/(l - r)$, and determined so as to be equal to the experimental value. The plastic strain corresponding to the applied stress can be evaluated from the stress-strain curve obtained by the tensile test. The left and right boundaries are assumed to be insulated, while the upper boundary is assumed to have a uniform current density of q to apply the macroscopic external current, which corresponds to the measured electric current in the above-mentioned experiment.

Since the electrochemical property of the damaged surface of stainless steel is unknown, we approximately use the polarization curves of SUS304 stainless steel and S50C carbon steel in 0.1% NaCl solution as the intact surface and damaged surface, respectively. These two curves are shown in Fig. 6, where the regression curve is also shown by the dotted line, and the regression function is empirically determined as

$$p = p_0 + R(i - i_0) + \frac{D}{1 + \exp[-(i - i_0)/B]}, \quad (10)$$

where R , D , B , p_0 and i_0 are the fitting constants determined individually for SUS304 and S50C. Note that the current density i denotes the outward current from the working electrode, and the current in the cathodic curve is negative. Meanwhile, in the BEM simulation, the

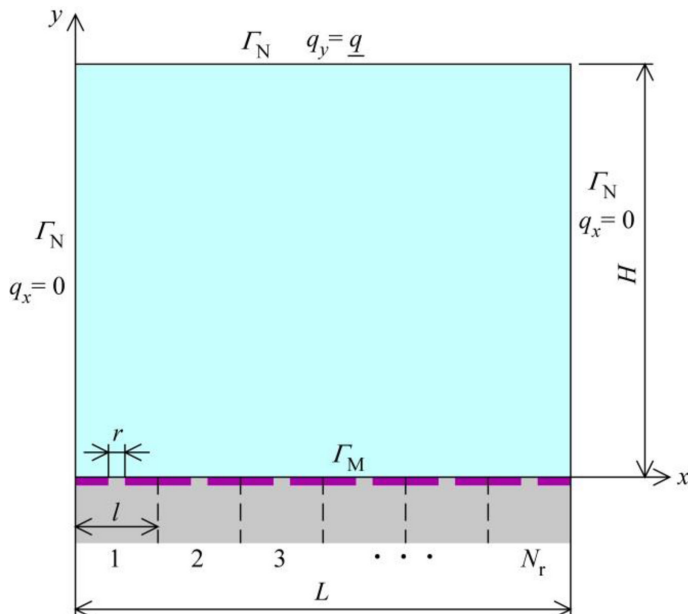


Figure 5: Simplified damaged passive film model.

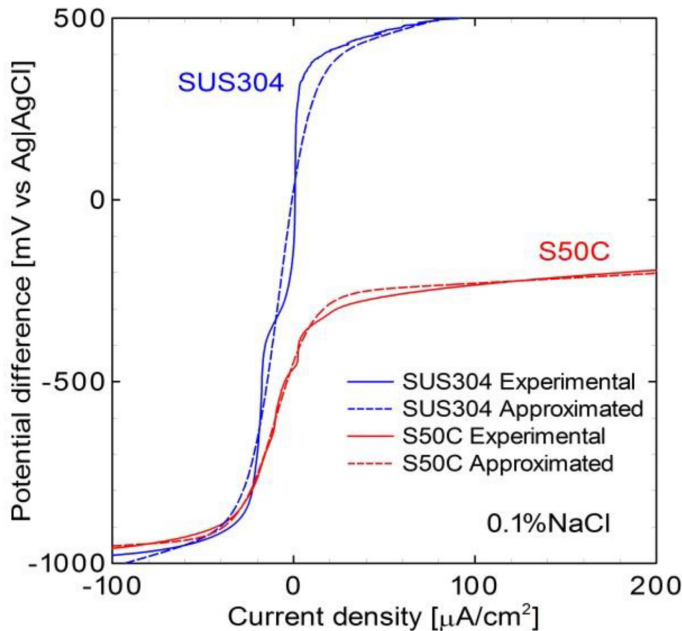


Figure 6: Polarization curves of SUS304 and S50C in linear scale.

outward current density denotes the current from the solution to the metal, so we need to invert the sign of the current density by $i = -\hat{q}$ and obtain

$$p = p_0 - R(\hat{q} + i_0) + \frac{D}{1 + \exp[(\hat{q} + i_0)/B]}. \quad (11)$$

At a node of an element in the metal boundary, the nodal potential and nodal current density follows eqn (11) of the corresponding material.

In the numerical examples, the total length of metal boundary is fixed to 1 mm, and the repetition number N is increased by shortening the unit length l to examine the convergence of solution when N approaches to infinity and the damage unit length l approaches to zero. After the examination on the size of damage unit, the unit length l is fixed to the sufficiently small value, and the external current \underline{q} is applied on the upper boundary to examine the variation of average potential on the metal boundary which corresponds to the measured potential difference in the experiment. By comparing the numerical and experimental results, we qualitatively examine the validity of the numerical simulation and discuss the effect of plastic strain on the corrosion electric field. The calculation results will be shown at the site of conference.

4 CONCLUDING REMARKS

The effect of stress on the polarization curve of stainless steel was discussed. The experimental results showed that the spontaneous potential decreased by the increase of applied stress. This is because the microscopic damage of the passive film yields a formation of new surface without passive film, and undermines the corrosion-resistance of the whole surface. To

evaluate this kind of microscopic damage effect on the corrosion behaviour, the damaged passive film model was proposed, and the BEM formulation was shown with the nonlinear polarization model.

ACKNOWLEDGEMENT

This work was financially supported by JSPS KAKENHI Grant Number 26289004.

REFERENCES

- [1] Revie, R.W. & Uhlig, H.H., *Corrosion and Corrosion Control*, 4th edn., John Wiley & Sons: New Jersey, pp. 92–96, 2008.
<http://dx.doi.org/10.1002/9780470277270>
- [2] Wagner, C., Contribution to the theory of cathodic protection. *Journal of the Electrochemical Society*, **99**(1), pp. 1–12, 1952.
<http://dx.doi.org/10.1149/1.2779653>
- [3] Waber, J.T., Mathematical studies on galvanic corrosion: I. Coplanar electrodes with negligible polarization. *Journal of the Electrochemical Society*, **101**(6), pp. 271–276, 1954.
<http://dx.doi.org/10.1149/1.2781244>
- [4] Strømmen, R.D., Computer modeling of offshore cathodic protection systems: method and experience. *Computer Modeling in Corrosion, ASTM STP 1154*, ed. R.S. Munn, American Society for Testing and Materials: Philadelphia, pp. 229–247, 1992.
- [5] Adey, R.A. & Niku, S.M., Computer modeling of corrosion using the boundary element method. *Computer Modeling in Corrosion, ASTM STP 1154*, ed. R.S. Munn, American Society for Testing and Materials: Philadelphia, pp. 248–264, 1992.
- [6] De Giorgi, V.G., Thomas II, E.D. & Kaznoff, A.I., Numerical simulation of impressed current cathodic protection (ICPP) systems using boundary element methods. *Computer Modeling in Corrosion, ASTM STP 1154*, ed. R.S. Munn, American Society for Testing and Materials: Philadelphia, pp. 265–276, 1992.
- [7] Aoki, S. & Kishimoto, K., Prediction of galvanic corrosion rates by the boundary element method. *Mathematical and Computer Modelling*, **15**(3–5), pp. 11–22, 1991.
[http://dx.doi.org/10.1016/0895-7177\(91\)90049-D](http://dx.doi.org/10.1016/0895-7177(91)90049-D)
- [8] Aoki, S. & Amaya, K., Optimization of cathodic protection system by BEM. *Engineering Analysis with Boundary Elements*, **19**(2), pp. 147–156, 1997.
[http://dx.doi.org/10.1016/S0955-7997\(97\)00019-2](http://dx.doi.org/10.1016/S0955-7997(97)00019-2)
- [9] Butler, B.M., Kassab, A.J., Chopra, M.B. & Chaitanya, V., Boundary element model of electrochemical dissolution with geometric non-linearities. *Engineering Analysis with Boundary Elements*, **34**(8), pp. 714–720, 2010.
<http://dx.doi.org/10.1016/j.enganabound.2010.03.007>
- [10] Butler, B.M., Chopra, M.B., Kassab, A.J. & Chaitanya, V., Boundary element model for electrochemical dissolution under externally applied low level stress. *Engineering Analysis with Boundary Elements*, **37**(6), pp. 977–987, 2013.
<http://dx.doi.org/10.1016/j.enganabound.2013.03.010>
- [11] Darowicki, K., Orlikowski, J., Arutunow, A. & Jurczak, W., The effect of tensile stresses on aluminium passive layer durability. *Electrochimica Acta*, **51**(27), pp. 6091–6096, 2006.
<http://dx.doi.org/10.1016/j.electacta.2005.12.054>

- [12] Krawiec, H., Vignal, V. & Szklarz, Z., Local electrochemical studies of the microstructural corrosion of AlCu_4Mg_1 as-cast aluminium alloy and influence of applied strain. *Journal of Solid State Electrochemistry*, **13**(8), pp. 1181–1191, 2009.
<http://dx.doi.org/10.1007/s10008-008-0638-8>
- [13] Orlikowski, J. & Darowicki, K., Electrochemical investigations of Al–Mg alloy subjected to tensile test. *Journal of Solid State Electrochemistry*, **13**(11), pp. 1659–1667, 2009.
<http://dx.doi.org/10.1007/s10008-008-0672-6>
- [14] Brebbia, C.A. & Dominguez, J., *Boundary Elements: An Introductory Course*, 2nd edn., WIT Press: Southampton, pp. 45–152, 1992.
- [15] Beer, G., Smith, I. & Duenser, C., *The Boundary Element Method with Programming*, Springer-Verlag: Wien, pp. 129–168, 2008.